ISSN 0016-8521, Geotectonics, 2015, Vol. 49, No. 4, pp. 302–319. © Pleiades Publishing, Inc., 2015.
Original Russian Text © V.S. Burtman, 2015, published in Geotektonika, 2015, No. 4, pp. 67–85.

# Tectonics and Geodynamics of the Tian Shan in the Middle and Late Paleozoic

**V. S. Burtman**
*Geological Institute, Russian Academy of Sciences, Pyzhevskii per. 7, Moscow, 119017 Russia*
*e-mail: vburtman@gmail.com*
Received April 28, 2014

**Abstract**—This work presents a model of the tectonic development and geodynamics of subduction processes of oceanic and continental crust, the formation of an accretionary prism, continental collision, the formation of the folded-nappe system, and the magmatic and sedimentation processes in the Tian Shan in the Middle and Late Paleozoic. Other models developed for this region are discussed.

*Keywords*: Tian Shan, Turkestan ocean, geodynamic model, nappe thrusts, strike-slip faults, oroclines, extrusions

**DOI:** 10.1134/S0016852115040020

## INTRODUCTION

Rocks of today's Tian Shan comprised several continental terranes separated by oceanic basins in the Middle Paleozoic (15). The Alai–Tarim and Kazakh–Kyrgyz terranes occupy an extensive area in the Tian Shan; Kara Kum and Bogdashan terranes occupy smaller areas (Fig. 1a). The Alai–Tarim, Kazakh–Kyrgyz, and Kara Kum terranes contain an ancient basement. The Late Carboniferous closure of the oceanic basins was followed by a continental collision. The latter initiated orogenic processes lasted up to the Permian. This work presents the model of development and geodynamics of these processes.

The following geographic provinces are distinguished in the Tian Shan: Western, Central, and Eastern (Chinese) (Fig 1b). To describe geological objects we use the modern system of coordinates.

## TERRANES

### *Bogdashan Terrane*

The Bogdashan terrane (Fig. 1) is separated by the West Junggar oceanic suture from the Kazakh–Kyrgyz terrane. This terrane comprises such ancient formations as Silurian siltstones and limestones, as well as Devonian volcanic–terrigenous and carbonate deposits [59, 89, 93]. The base of the observable section of the Bogdashan terrane is mainly made of Carboniferous formations (tuffogenic, chert, and carbonate–clastic turbidities with interlayers of volcanic rocks [44]. Volcanic rocks, contrasting in their composition, are represented by basalts, rhyolites, and pyroclastics. Basalts are present in pillow, tholeiitic, and high-Ti varieties. The isotope ages of the basalts are 320 and 354 Ma. The REE distribution in basalts indicates their intraplate origin, on the one hand, and their genesis over a zone of subduction, on the other [33, 95]. The carboniferous formations are penetrated by intermediate and mafic intrusions. The U–Pb ages of granodiorite and diorite-trondhjemite from the Bogdashan Range are 345 and 328 Ma, correspondingly [58]. The section of the Lower Carboniferous deposits in the Ilinkhabirga mountains is composed of felsic volcanic rocks, volcanogenic–clastic, and carbonate deposits; the Upper Carboniferous section is represented by flysch deposits [89, 93].

By the Middle Paleozoic the Bogdashan terrane was an island arc in the paleo-Asian ocean, separated the West Junggar marginal basin, which was closed in the Late Carboniferous or Early Permian [55, 84]. In the Ilinhabirga Mountains the Late Carboniferous island arc deposits are discordantly overlain by the Late Permian to Early Triassic continental molasse deposits [89, 93].

### *Kara Kum Terrane*

Most of the Middle Paleozoic Kara Kum continental terrane (named also: Kara Kum–Tadzhik, Turan) lies beyond the Tian Shan. The evolution of the Kara Kum terrane in Middle Paleozoic was similar to that of the Alai–Tarim terrane, since the former was a constituent of the terrane. The structures of the Kara Kum and Alai–Tarim terranes are separated by the Hissar oceanic suture (Fig. 1), which probably was a rift branch of the Kunlun–Gindukush paleo-Thetis ocean [14, 15].

The Hissar rift was emplaced in the Early Carboniferous. Rift volcanism began in the Late Tournasian. The oceanic crustal rocks are categorized as Late Serpuchovian, Bashkirian, and Early Moscovian [29]. During Moscovian and Casimovian Stages there was

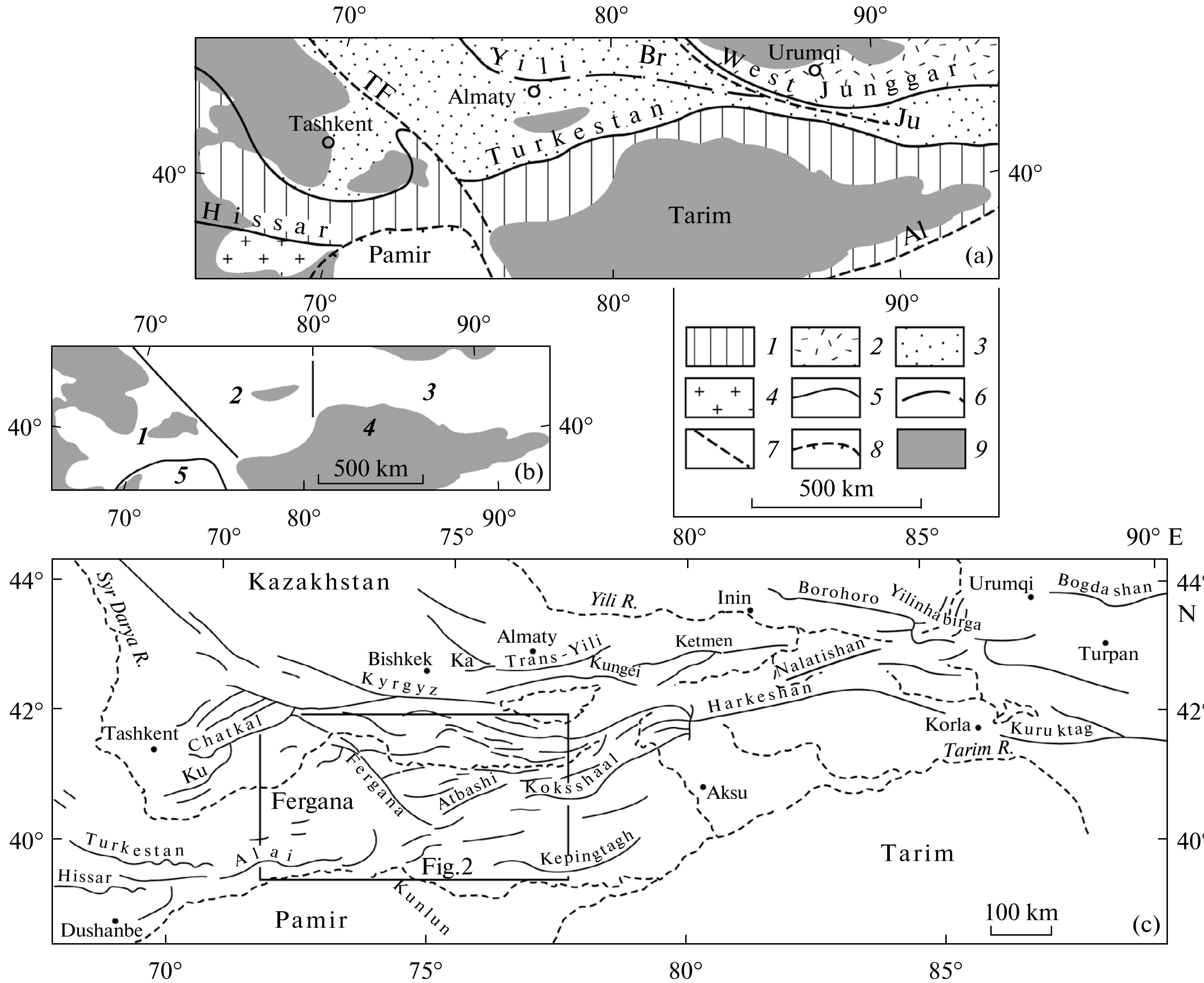


**Fig. 1.** Middle Paleozoic terranes and geographic provinces of the Tian Shan. (a) Continental terranes (*1–4*): (*1*) Alai–Tarim, (*2*) Bogdashan, (3) Kazakh–Kyrgyz (Br means Borohoro Block), (*4*) Kara Kum; (*5*) and (*6*) oceanic sutures: (5) Late Paleozoic, (*6*) Middle Paleozoic; (7)fault zones (Al, Altyntagh; Ju, Junggar; TF, Talas–Fergana); (*8*) Cenozoic tectonic boundary of Pamir; (*9*) Cenozoic depressions. (b) Geographic provinces (*1–5*): (*1*) Western Tian Shan, (*2*) Central Tian Shan, (*3*) Eastern Tian Shan, (*4*) Tarim, (*5*) Pamir. The distribution area of Cenozoic rocks is shown in gray. (c) Mountain ranges, mentioned in the text: Ka, Kastek; Ku, Kurama.

an accumulation of turbidites in the Hissar basin. During the Casimovian–Gzhelian the collision of the Kara Kum and Alai Tarim terranes led to the closure of the Hissar oceanic basin.

### *Alai–Tarim Terrane*

The Alai–Tarim terrane comprises the ancient Tarim massif (craton), occupying the depression of the same name, and an area at the periphery of the massif, intensively deformed in the Phanerozoic. Only part of the massif, deformed in the Paleozoic and Cenozoic, is located within the Tian Shan. In the north, the terrane is bounded by the Turkestan (South Tian Shan) oceanic suture, which closed in the Late Carboniferous [14, 15]. The southern boundary of the terrane is more complex and includes several components (from the southeast to the west): the Paleozoic Kunlun oceanic suture (closed in the Triassic), the tectonic boundary of the Cenozoic Pamir allochthon, and the Paleozoic Hissar oceanic suture (Fig. 1).

The Turkestan margin (facing the Turkestan Ocean) of the Alai–Tarim Paleozoic continent was passive. It is distinguished into two zones: namely, the Inner and Outer facies zones (Figs. 2, 3). The total width of these zones before the Late Paleozoic overthrusting and folding may have reached 500 km. In the Silurian, pelagic terrigenous and siliceous–terrigenous sediments accumulated on the continental slope in both facies zones. Apart from turbidites, silty–pelitic formations (deposits of apical parts of mud flows) are widespread. Short-term outpourings of volcanic rocks of mafic, intermediate, and felsic composition, associated with ruptures of

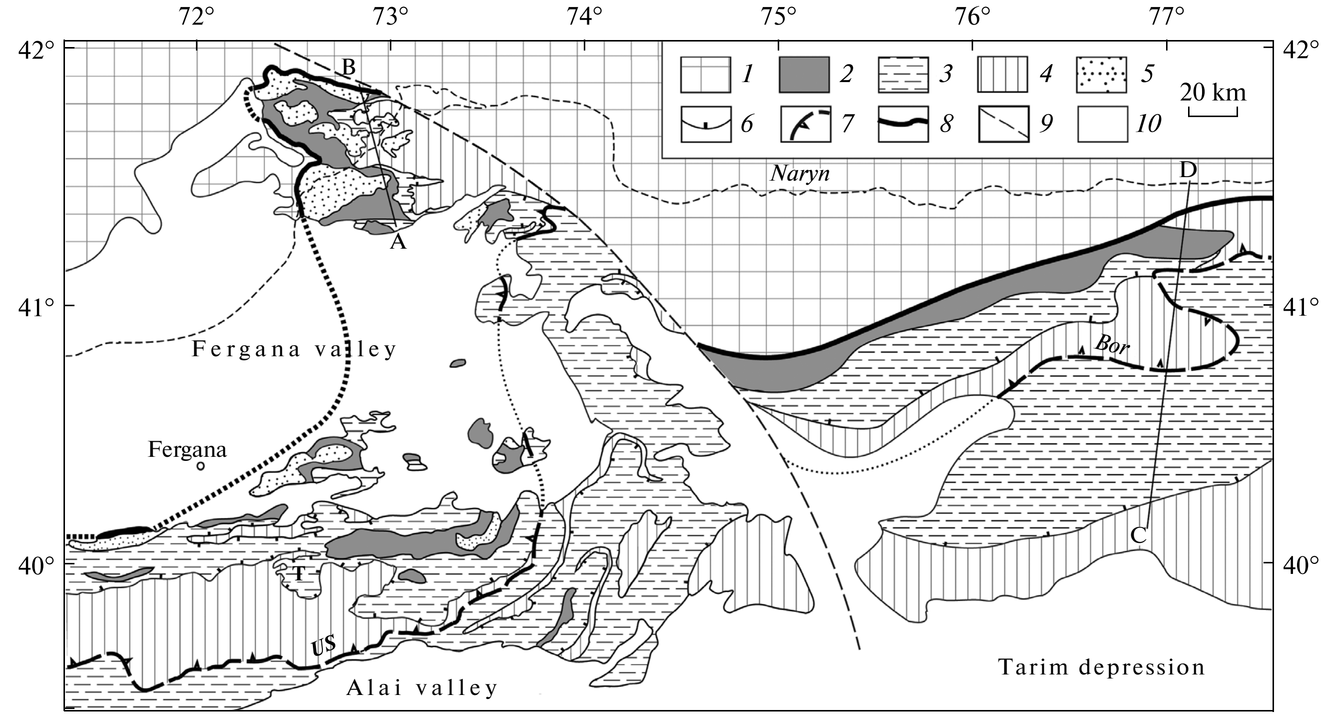


**Fig. 2.** Alai–Tarim terrane in Western and Central Tian Shan. (*1*) Kazakh–Kyrgyz terrane; (*2–5*) Alai–Tarim terrane: (*2*) tectonic plates including oceanic crustal rocks in upper and middle levels of the ensemble of primary nappes, (*3*) rocks of the outer zone of the Alai–Tarim terrane at the lower level of primary nappes (T means Tegermach nappe), (*4*) Inner zone of the Alai–Tarim terrane (primary allochthon), (*5*) neoautochthons; (*6–9*) fault zones: (*6*) tectonic base (overthrust fault) of nappes of the lower level, (*7*) major secondary overthrust faults (US, Uzgen–Sanzar; Bor, Borkoldoi), (*8*) post-collision South Tian Shan fault, suture of the Turkestan ocean, (*9*) Talas–Fergana fault; (*10*) Cenozoic and Mesozoic rocks.

this passive margin were to be found within some areas. Volcanic buildups became the base for development of limestone reefs in the Late Silurian.

In the Late Silurian–Devonian the inner zone was uplifted up to the neritic level with synchronous accumulation of carbonate sediments. Carbonate sedimentation terminated in different areas at different times within the interval from the Bashkirian to Asselian (Fig. 3I). In some localities the sedimentation processes was accompanied by intraplate rift volcanism. In the Serpukhovian and later, silicites appeared among carbonate rocks. During the gradual closure of the Turkestan oceanic basin, which preceded the collision of the Alai–Tarim and Kazakh–Kyrgyz terranes, the inner zone of the Alai–Tarim was submerged into the zone of pelagic sedimentation with accumulation of turbidites. This happened in different areas of the zone at different times within the interval from the Late Bashkirian to Asselian.

The outer zone was characterized by pelagic sedimentation in the Devonian and Early Carboniferous (Fig. 3II). Deposits, including dominating silica rocks, were slowly accumulating on the flat continental slope for a long period of time. These deposits comprise condensed stratigraphic sections. The sedimentation rate in some sections was only 1 mm per 1000 years [14]. In the Late Early Carboniferous, turbidities were deposited within the outer zone.

### *Kazakh–Kyrgyz Terrane*

The Kazakh–Kyrgyz Middle Paleozoic continental terrane (named also: Kazakhstan, Kyrgyz, Kazakh–Yili) formed as a result of the combination of

**Fig. 3.** Stratigraphic columns of structural units of the ensemble of primary nappes of the Southern Tian Shan: (I) Inner zone of the Alai–Tarim terrane (autochthon), (II) rocks of the outer zone of the Alai–Tarim terrane in nappes of the lower level, (III–IV) rocks of oceanic crust and accretionary prism in nappes of the middle (III) and upper (IV) levels. (*1*) continental deposits; (*2*) conglomerates and breccias at the base of neoautochthon; (*3*) carbonate deposits of the shelf zone; (*4*) limestones with chert nodules, deposited at the deep part of the shelf zone; (*5*) volcanogenic-terrigenous and volcanic rocks of the zones of shelf and continental slope; (*6*) terrigenous and siliceous-terrigenous deposits, accumulated on the continental slope and its base (flysch, olistostrome); (*7*) stratigraphically condensed carbonate-silica and silica deposits, accumulated on the continental slope and oceanic floor; (*8–9*) oceanic basalts, hyaloclastites, ignimbrites: (*8*) weakly altered, (*9*) metamorphosed; (*10*) time of overthrusting; neo means neoautochthon. Structural units, after [14, 41]: *Abshir*, *Atbashi*, *Baubashata*, *Isfayram*, *Kan*, *Keltubek*, *Kerey*, *Kokkija*, *Maydantag*, *Muzduk*, *Ontamchi*, *Taldyk*, *Chatyr Kul*, *Shaidan*, and *Shankol*.

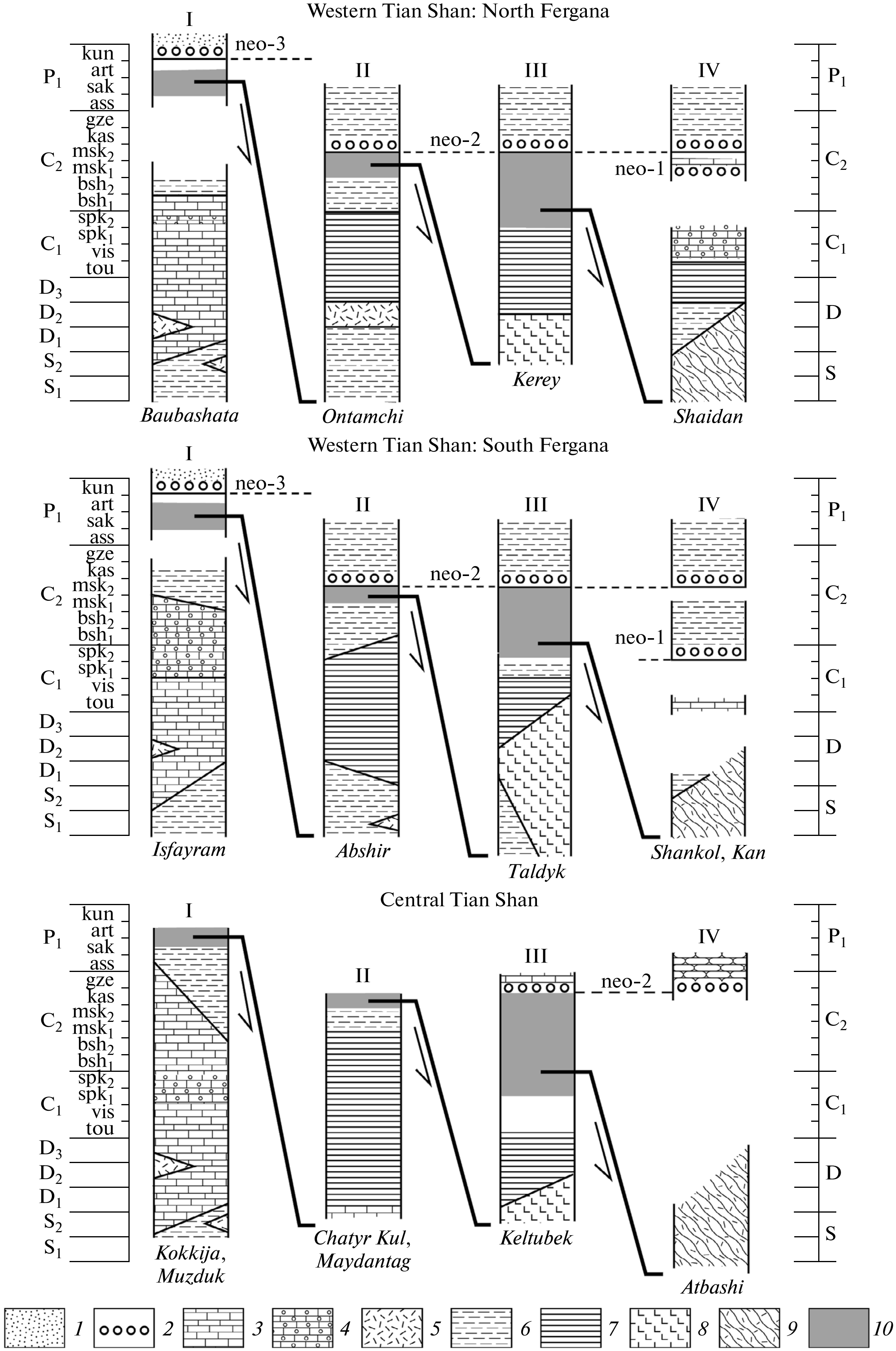
Western Tian Shan: North Fergana
I
II
III
IV
neo-3
neo-2
neo-1
kun
art
sak
ass
gze
kas
msk2
msk1
bsh2
bsh1
spk2
spk1
vis
tou
P1
C2
C1
D3
D2
D1
S2
S1
D
S
Baubashata
Ontamchi
Kerey
Shaidan
Western Tian Shan: South Fergana
Isfayram
Abshir
Taldyk
Shankol, Kan
Central Tian Shan
Kokkija, Muzduk
Chatyr Kul, Maydantag
Keltubek
Atbashi
1
2
3
4
5
6
7
8
9
10

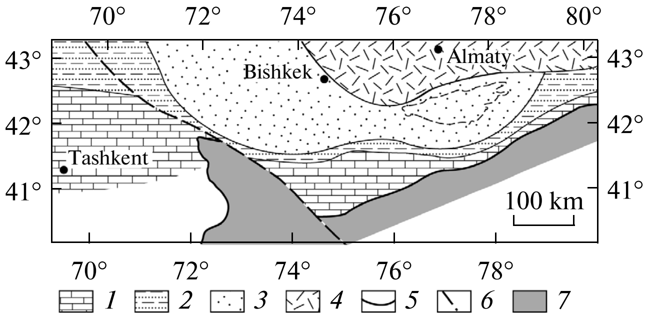


**Fig. 4.** Kazakh–Kyrgyz terrane: Early Carboniferous deposits in West and Central Tian Shan. (*1*) carbonate deposits; (*2*) carbonate-terrigenous deposits; (*3*) continental clastic rock-dominating sediments; (*4*) volcanic-terrigenous continental deposits (Trans-Yili magmatic province); (*5*) Turkestan oceanic suture; (*6*) Talas–Fergana fault; (*7*) Alai–Tarim terrane.

the Issyk-Kul and Syr Darya Early Paleozoic terranes. This happened in the Ordovician after the closure of the Terskey oceanic basin, separated above terranes in the Early Paleozoic [14, 15, 40].

### *Silurian and Devonian*

In the Early Silurian the Kazakh–Kyrgyz continent was situated between the Turkestan and Yili oceanic basins. After the closure of the Yili oceanic basin [14, 15], the sialic block Borohoro became a part of the Kazakh–Kyrgyz continent (Br, Fig. 1). In the Devonian and Carboniferous the Tian Shan part of the Kazakh–Kyrgyz continent was located between the Turkestan and West Junggar oceanic basins.

In the Early Silurian, flysch deposits accumulated on the continental slope, carbonate deposits in the outer shelf zone, carbonate-terrigenous deposits in the inner shelf zone of the Kazakh–Kyrgyz continent. Among Lower Silurian terrigenous deposits are subduction-related intermediate and felsic effusives. The latter were deposited also on the Borohoro microcontinent in the Early Silurian [59, 75].

Higher in the stratigraphic succession of West Tian Shan are Late Silurian–Eifelian continental volcanogenic and volcanogenic–terrigenous deposits. Volcanic rocks are composed of (from bottom to top): basalts, trachybasalts, andesitobasalts, andesites, and trachyandesites in the lower part of the sequence to rhyolites and trachyrhyolites in the upper part. The $K_2O$ content in effusives of the same silica acidity increases in the northward direction. Upward in stratigraphy, the volcanic explosivity index decreases and the amount of volcanic rocks increases. These temporal variations are determined by subsequent subduction of oceanic crust beneath the Turkestan oceanic basin. The Rb–Sr isochrone ages of andesite and trachyandesites lavas are $426 \pm 4$ and $422 \pm 4$ Ma; the ages of gabbroid and alaskite intrusions, comagmatic to volcanic rocks, are $409 \pm 25$ and $418 \pm 4$ Ma, correspondingly [2].

In the Givetian and Late Devonian, continental molasse and marine shallow-water carbonate–terrigenous and carbonate deposits were deposited on the Turkestan margin of the Kazakh–Kyrgyz terrane. In the Trans-Yili area of the Central Tian Shan comprising the Trans-Yili, Kungei, and Kastek ranges, the Givetian and Franian stages are represented by continental volcanogenic–terrigenous deposits. The lower part of the stratigraphic succession is composed of andesite lava and tuff lava with interlayers of basalts, dacites, tuffs, and sandstones; the upper part of the succession is made of rhyolites, dacites, tuff lavas, and tuff sandstones. The U–Pb zircon ages of granite massifs associating with volcanites are in interval of 390–414 Ma [21, 78]; the Rb–Sr isochrone age is 365 Ma [60]. These and older rocks are overlain by Late Devonian orogenic red molasse deposits.

The Devonian magmatism in the Trans-Yili area is considered a branch of the Devonian Kazakhstan volcanic belt and associated with subduction of the Junggar–Balkhash oceanic basin [8, 31, etc.]. These conclusions are debatable. The zone of Devonian magmatism extends in the western direction from the Trans-Yili area towards the Kyrgyz Range, where Devonian volcanic rocks and granites are widespread. To the east of the Trans-Yili area in the Nalatishan Range near the Turkestan oceanic suture the Middle Paleozoic I-type granites, including Devonian granites (U-Pb age, 400 Ma), are widespread. The latter are overlain transgressively by Lower Carboniferous deposits [59, 75]. The Devonian magmatic belt, occupying the territory of Nalatishan, Kungei, Trans-Yili, and Kyrgyz ranges, is located close to the Turkestan suture, but not to the Junggar one. The formation of this magmatic belt is probably associated with subduction of the lithosphere of the Turkestan oceanic basin. The distance from the magmatic belt to the Turkestan suture varies due to the uneven tectonic shortening of the territory of Tian Shan during the Late Paleozoic orogenesis and probable variations in dip angles of the subduction zone.

### *Carboniferous*

In the Western and Central Tian Shan on the Turkestan margin of the Kazakh–Kyrgyz continent, shallow-water carbonate deposits accumulated in the Early Carboniferous. In the Turnesian evaporites accumulated in lagoons; in the Visean, carbonate mud was added by a significant admixture of siliceous material. The zone of neritic limestones is more than 100 km wide in the west and decreases to 15–20 km to the east of the 75° meridian (Fig. 4). In the zone of carbonate–terrigenous deposits, located to the north, the sedimentation regime was unstable and laterally uneven throughout the territory. There are coarse-grained, coastal, lagoon, and turbidite deposits [14, 32].

The intracontinental area, which occupied a vast territory in Central Tian Shan, was a flat eroded land in the Tournaisian and the most of the Visean. Only the eastern side of the Kyrgyz Range was occupied by a shallow marine basin, where clastic rocks and carbonaceous pelites accumulated. In the Late Visean to Early Serphukhovian, the inner part of the terrane was characterized by accumulation of red terrigenous clastic alluvial deposit. The lowland was periodically flooded, that is confirmed by the occurrence of carbonate rocks containing shallow marine fauna remains among the continental deposits.

The first signs of magmatic activity are noted in Serpukhovian deposits of the Chatkal–Kurama area of the Western Tian Shan. Limestones containing Serpukhovian fauna interbed with trachybasaltic tuffs and lavas. During the Late Carboniferous multikilometer volcanic strata accumulated in the Chatkal–Kurama area under mostly land conditions, later being intruded by granites. Trachybasalt, trachyandesite, and trachydacite lavas (the Minbulak and other formations) erupted during the Bashkirian. The Rb–Sr isochrone age of these volcanic rocks 317 ± 6 Ma; the Rb–Sr age of granites is 316 Ma [18]. In the Moskovian and Kasimovian Casimovian ages, trachyandesite, andesite, dacite, and rhyolite (Nadak and other formations) lavas outpoured; the Rb–Sr isochrone age of these rocks is 298–300 Ma [18]. Petrochemical data indicate the subduction-related nature of Carboniferous magmatism in the Chatkal–Kurama area.

In the Central Tian Shan (the Trans-Yili area) intense volcanic eruptions occurred in Early and Late Carboniferous. Terrestrial volcanism dominated. Intrusive rocks of the Central Tian Shan are represented by granite, granodiorite, granosyenite, adamellite, gabbro, gabbronorite, and monzonite. The Rb–Sr isochrone age of alkaline rocks are in a range of 296–326 Ma [60].

The entire territory of the Kazakh–Kyrgyz continent in the East Tien Shan was characterized by intensive volcanism in the Carboniferous. Volcanic rocks belong to the calc-alkaline series; their geochemical parameters indicate subduction-related settings of the formation [90]. In the Eastern Tian Shan and Turkestan–Junggar, active margins of the Kazakh–Kyrgyz terrane were close to each other. Due to this, it is difficult to identify the position of the boundaries between the subduction-related volcanism zones of these active margins. The pattern of development of intrusive magmatism is easier to understand. In the Eastern Tian Shan there are numerous I-type granite intrusions, which form two magmatic belts. The belt in the Nalatishan Range located near Turkestan oceanic suture; the intrusive belt, a part of the Borohoro Range, extends along the West Junggar oceanic suture structure.

The intrusive belt Nalatishan is of composed of Devonian and Carboniferous granites and volcanic rocks. The stratigraphic Lower Carboniferous succession (from bottom to top) is as the following: dacites, rhyolites, and sandstones (the lower part), andesites, trachyandesites, tuffs, and basalts, probably, of rift origin (the upper part) [95]. The Rb–Sr age of granites associated with Early Carboniferous volcanites is 340 Ma. The potassium content in granites increases northward as the distance from the Turkestan suture increases [59, 75]. The magmatic belt continues in westerly direction towards the Trans-Yili region of Central Tian Shan.

Carboniferous volcanoclastic sediments and granites are common in the Borohoro magmatic belt. The Rb–Sr isochrone age and the Ar–Ar age of andesites are 345 ± 9 and 325 ± 1 Ma [90], correspondingly; the Ar–Ar age of adakites are 310–306 Ma [84]. The U–Pb ages of granites and granite-diorites are in the range of 366–341 Ma [84] and 315–301 Ma [55]. REE ratios indicate the subduction-related genesis of granites; the potassium content in the granites increases in the southeastern direction with increasing distance from the West Junggar oceanic suture [59]. In the northwesterly direction, this magmatic belt continues into the Kazakhstan territory of the Junggar Range.

Both margins of the Kazakh–Kyrgyz continent were active in the Middle Paleozoic. The age of ophiolites [14] shows that the spreading in the Turkestan Ocean occurred in the Silurian and Early to Middle Devonian. Subduction-related magmatism within the Kazakh–Kyrgyz terrane confirms the pattern of oceanic crust subduction beneath the Kazakh–Kyrgyz continent at this time. These processes are likely to have terminated in the Late Devonian. The subduction of oceanic crust began again in the Late Early or Late Carboniferous [14] and the Turkestan oceanic basin began to narrow. This oceanic basin was closed in the Late Carboniferous.

During the Carboniferous, the oceanic crust of the West Junggar Basin subducted beneath the Kazakh–Kyrgyz continent in the northeastern margin of the Kazakh–Kyrgyz continent. The West Junggar oceanic basin was closed in the Late Carboniferous or Early Permian [14, 15, 55, 84].

### *Accretionary Prism on the Margin of the Turkestan Oceanic Basin*

In the Middle Paleozoic, an accretionary prism formed on the Turkestan margin of the Kazakh–Kyrgyz continent. The fragments of the accretionary prism belonging to the continent were overlapped by flysch and terrigenous deposits (the neoautochthon-1; Fig. 3). The neoautochthon-1 rocks of the Western Tian Shan are in an age range from the Serpukhovian Stage to the Late Moscovian Substage. The formation of the accretionary prism was terminated at the beginning of the collision between the Alai–Tarim and the Kazakh–Kyrgyz continental terranes. Rocks comprising the accretionary prism now belong to the allochthon of the Alai–Tarim terrane (Figs. 2, 3).

The accretionary prism is composed of rocks of different origins. Among them are Turkestan oceanic

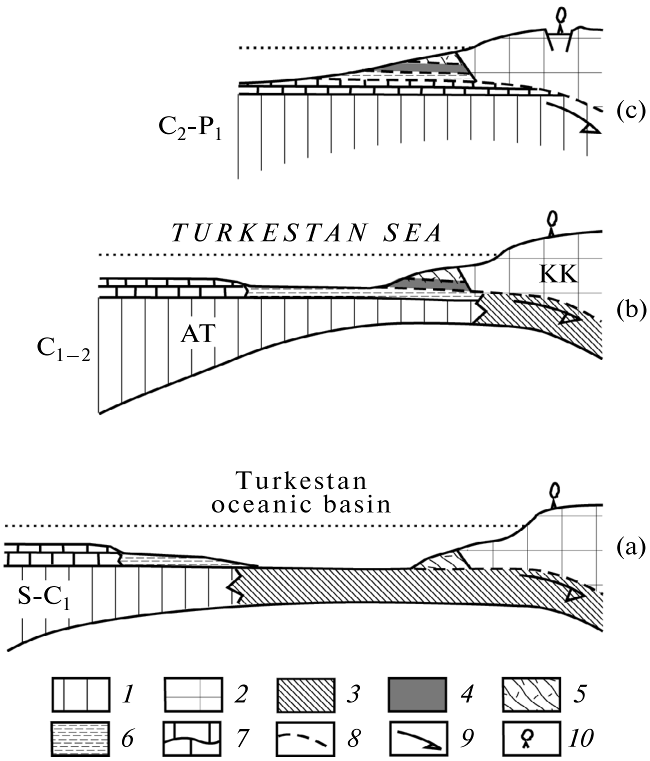


**Fig. 5.** Scheme of emplacement of tectonic sheets of upper (a), middle (b), and lower levels of the ensemble of primary nappes of South Tian Shan. (*1*, *2*) continental crust of the Alai–Tarim (*1*) and Kazakh–Kyrgyz (*2*) terranes; (*3*) oceanic crust; (*4*, *5*) allochthons, comprising weakly altered (*4*) and metamorphosed (*5*) oceanic crustal rocks; (*6*, *7*) rocks of Outer (*6*) and Inner (*7*) zones of the Alai–Tarim terrane margin; (*8*) tectonic boundaries; (*9*) direction of subduction of the oceanic and continental lithosphere; (*10*) manifestations of volcanism.

crustal rocks, metamorphosed under high-pressure metamorphic conditions, being subducted and then exhumed on the Earth's surface. Some of these rocks, during or after exhumation, were subjected to blue and green schist retrogressive metamorphism. In the Atbashi Range (Central Tian Shan) common blue schists and eclogites are unconformably overlain by terrigenous–carbonate deposits, containing Upper Carboniferous (Gzhelian) fusulinids [57]. The Sm–Nd isochron age of eclogite is 319 ± 4 Ma [57]; the Ar–Ar phengite and glaucophane ages are in the range of 324–327 Ma [30] and 316 ± 3 Ma [57], correspondingly. The Rb–Sr isochrone age of eclogite was 267 ± 5 Ma [83], which may be underestimated due to the fluid impact on the rock [49, 88].

For the eastern Tian Shan, the following age datings were obtained: Ar–Ar glaucophane and phengite ages of eclogite metamorphism are 364 ± 2 and 401 ± 1 Ma, correspondingly [98], the Sm–Nd isochrone eclogite age is 343 ± 44 Ma [51]. The U–Pb rutile and zircon ages of eclogite are 318 ± 7 Ma [67] and 413–310 Ma, correspondingly [53, 82]. The Lu–Hf isochrone age of garnets in rocks that were metamorphosed under the HP metamorphism is 315 ± 1 Ma [64]. The U–Pb ages of zircon rims from eclogites are 233 ± 4 and 226 ± 5 Ma, respectively [98], but the relationship of these age datings with high-pressure metamorphism is still debatable [82, 88]. The Ar–Ar age of the blue schist metamorphism from crossite, glaucophane, and phengite is in the range of 344–347 Ma [51]. The Rb–Sr and Ar–Ar ages of retrograde metamorphism obtained on white mica are in the range of 302–313 [63] and 316–331 Ma [88].

Isotopic ages of eclogite metamorphism indicate that conditions for high-pressure metamorphism and exhumation of metamorphic rocks existed, probably repeatedly, over a considerable age interval. The ages of high-pressure metamorphic (except for problematic age datings) and retrograde metamorphism are older than 300 Ma. This age limit corresponds to the time of the collision of the Alai–Tarim and the Kazakh–Kyrgyz terranes.

## COLLISION BETWEEN THE ALAI–TARIM AND KAZAKH–KYRGYZ TERRANES

The subduction of the Turkestan oceanic crust beneath the Kazakh–Kyrgyz terrane was followed by a collision between the Alai–Tarim and the Kazakh–Kyrgyz terranes. According to geological data, the beginning of collision was in the age interval of 310–300 Ma: in the West and Central Tian Shan, in the Moscovian and Casimovian (Fig. 3), and in the eastern Tian Shan, probably in the Gzhelian [1]. The onset of the collision resulted in the change of subduction of the Turkestan oceanic crust by the subduction of the Alai–Tarim continental crust beneath the Kazakh–Kyrgyz continent (Fig. 5).

Continental collision was accompanied by deformation processes resulting in the formation of a fold–nappe belt extending along the suture of the Turkestan Ocean. A geodynamic pattern of the collision process [13, 38, 39] has been interpreted on the basis of the results of geological mapping of the study area and paleontological age determinations of rocks. Owing to subsequent investigations, the isotopic ages of magmatism and metamorphism as well as geochemical data on the origin of igneous rocks were obtained. These data require the pattern to be revised. They also contribute arguments in its favor.

### *Collisional Deformation*

#### *First stage*

The first stage of the collisional deformation led to the formation of a system of nappes, which together with the deformed autochthon form the Southern Tian Shan fold–nappe tectonic zone [7, 12–14, 28, 38, 41]. The latter occupies a part of the Tian Shan located south of the Turkestan Ocean suture.

After the closure in the Late Carboniferous of the oceanic crustal part of the Turkestan Basin, marginal parts of terranes with thin continental crust remained under water, where flysch deposits alternating with olistostrome horizons accumulated. Nappes formed on the crast of the Alai–Tarim terrane at the bottom of the Turkestan intracontinental sea, which was the successor of the Turkestan paleoocean. Sedimentation was terminated in areas overlapped by nappes, continued on the moving tectonic plates, and in front of thrusts. The formation of nappes started in the Moscovian and continued interruptedly from 20–25 Ma up to the Sakmarian or Artinskian. Granites that intruded autochthonous and allochtonous structures have an Artinskian isotope age [1, 78].

Upper nappes are made of rocks of the accretionary prism (Fig. 3IV), which formed in the Turkestan oceanic basin at the margin of the Kazakh–Kyrgyz continent in the Middle Paleozoic and Early Carboniferous (Fig. 5a). Apart from other rocks of the accretionary prism there are metamorphosed ophiolites.

During the subduction of the Turkestan oceanic crust, the plates of weakly altered ophiolites were detached from the top of the subducting slab. Tectonic plates containing such ophiolites (Fig. 3III) were thrust under the metamorphic rocks of the accretionary prism (Fig. 5b), forming the middle level of the ensemble of thrust nappes.

During the Late Carboniferous collision, the outer zone of the Alai–Tarim continent (Fig. 3II) was thrust under ophiolite nappes (Fig. 5c). At that time, or later, rocks of the Outer Zone of the Alai–Tarim continent were tectonically layered. The separation surface was confined to the Silurian shales of this zone. During the ongoing continental subduction the Inner zone of the Alai–Tarim terrane (Fig. 3I) have been underthrusted beneath a detached sedimentary complex of the Outer zone in the Sakmarian–Artinskian, but this could have began earlier (Fig. 3). The overthrusting process was accompanied by the deformation of rocks inside tectonic sheets and formation of ensembles of recumbent folds in the flysch strata [14].

The processes described formed a three-level ensemble of primary thrust nappes. Thrust nappes of the upper level contain metamorphosed rocks of the oceanic crust and accretionary prism; the middle level contains slightly altered ophiolites; the lower level is composed of rocks of the outer zone of the Alai–Tarim terrane. The inner zone of the Alai–Tarim terrane was autochthon. The results of studying the vergence of folds in the Tegermach nappe in the West Tian Shan (Fig. 6) show that the allochthon is displaced in the southern direction relative to the autochthon. This is also confirmed by the vergence of folds in primary nappes of Eastern Tian Shan [1] and the Kyzyl Kum [12]. At the end of the first stage of deformation, there was partial tectonic juxtaposition of the ensemble of nappes, including the primary autochthon. In the Western Tian Shan the Uzgen Sanzar overthrusting was the most important; in the Central Tian Shan it was the Borkoldai overthrusting (Fig. 2), the magnitude of which is in the tens of kilometers.

### *The second stage*

The formation of the ensemble of thrust nappes was followed by submeridional shortening of the Tian Shan. At this stage, the tectonic deformations spread to the territory not affected by the overthrusting, and there was change in the pattern and kinematics of deformations. As a result, nappes and autochthon were a system of large synform and antiform folds (Fig. 7, 8). As a result of the folding the submeridional shortening of the Southern Tian Shan tectonic zone by 25–50% took place [76]. The folds formed in Southern Tian Shan at this stage of deformation are often inclined or overturned to the north, toward the Turkestan suture. The overturned folds are accompanied by north-vergent small overthrusts and nappes [14]. The second stage of deformation occured in the Late Early Permian and Late Permian.

Collision deformations have the same structural patterns throughout the fold belt of the Tian Shan and Kyzyl Kum, laterally over 2500 km. Folds and overthrusts were formed in the upper crust, which was detached from the lower crust. The reduction of the lower crustal area of the Alai–Tarim terrane was probably a result of its subduction beneath the Kazakh–Kyrgyz terrane.

### *Post-Collision Deformations*

In contrast to the collision deformation pattern, post-collision deformations were different in different parts of the fold belt. These processes took place in the Permian and, probably in the Early Triassic. The pattern of post-collision deformations in the study area is determined by horizontal folds (oroclines) and strike-slip faults. The dominant structural forms are the Talas-Fergana fault, the Fergana horizontal flexure, and the Junggar strike-slip fault.

### *Talas–Fergana Strike-Slip Fault*

The dextral strike-slip along the Talas–Fergana fault (Figs. 1, 3, 4) led to the displacement of facies and tectonic zones, plutonic rocks, and folds [11, 39]. The magnitudes of horizontal displacement of *Middle Paleozoic, Late Carboniferous and Early Permian* geological formations are the same. The displacement occurred after their formation. The main shear displacement along the Talas–Fergana fault occurred in the Late Permian to Triassic. During the shear displacement the crystallization of phengite (Ar–Ar age of 246–260 Ma) probably occurred in mylonites of the Talas-Fergana fault [77]. The dextral shear displacements along the Talas–Fergana fault occurred in the Jurassic and in the Cenozoic [11, 16, 43]. The Talas-Fergana fault crosses the Tian Shan in the NW–SE

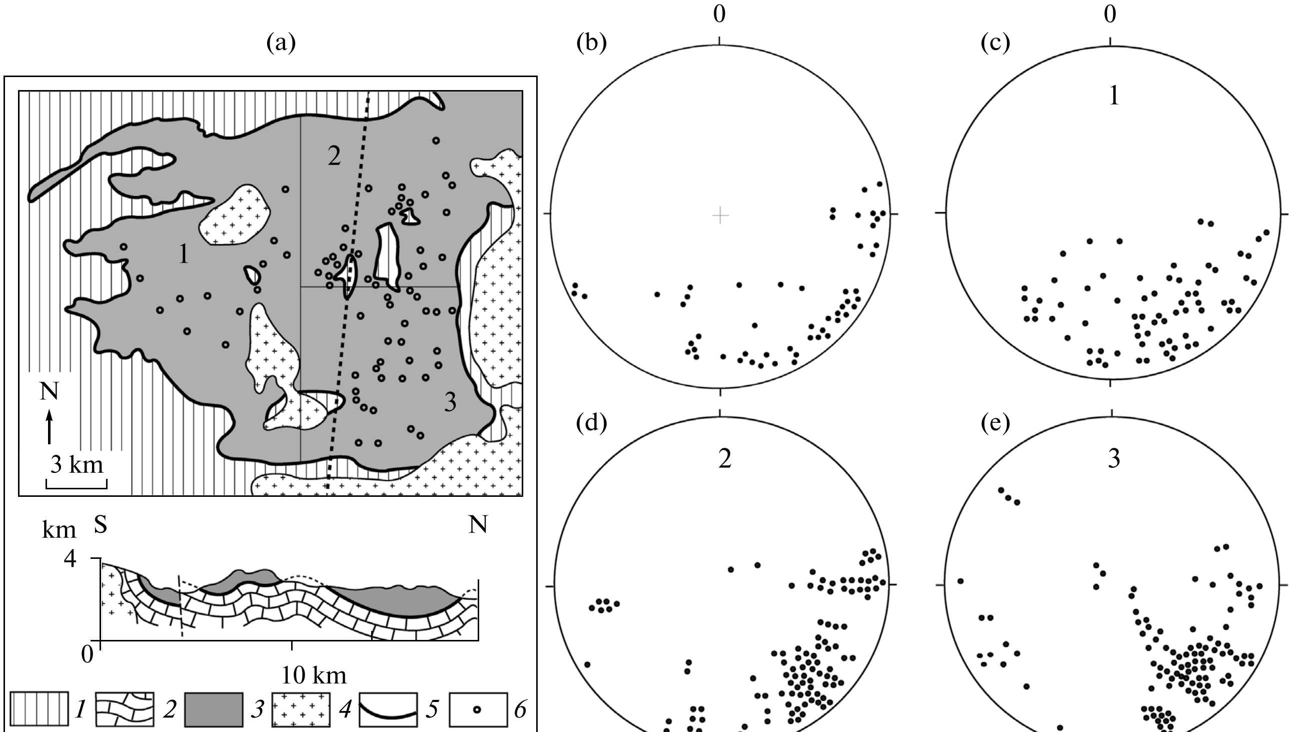


**Fig. 6.** Vergence of folds in the Tegermach nappe (the lower level of the ensemble of primary nappes). (a) The geological map of the Tegermach nappe (T in Fig 2): (*1*, *2*) autochthon, Carboniferous rocks: (*1*, on the map, *2*, on the section); (*3*) allochthon, Silurian flysch; (*4*) granites; (*5*) the base of allochthon (overthrusting fault); (*6*) sites of studying the folding. (*1–3*) sectors of the nappe; boundaries are marked by thin lines; the dashed line shows the line of the geological section. (b)–(e) Stereograms of folds vergence, resulted from the overthrusting at the first stage of the collision deformation (polar equidistant projection with points of intersections of axial fold planes with the upper hemisphere): (b) vergence of 53 isoclinal folds in modern system of coordinates, (c)–(e) vergence of 289 isoclinal and compressed folds in nappe sectors 1–3 after introduction of correction. The latter exclude deformation of the allochthon at the second stage of the collision deformation; number of folds in nappe sectors: 1–71, 2–107, 3–111; folds vary in size from 0.5 to 500 m.

direction. In Late Paleozoic the fault zone extended to the southeast along the western margin of the Tarim craton [11, 42, 43, 77].

Folds and faults formed during the collision deformation were transformed into horizontal folds oriented towards each other on opposite wings of the Talas–Fergana fault. The highest magnitude (180 km) of the Talas–Fergana strike-slip fault is noted in its northern part. With regard to plastic deformation, during the formation of horizontal folds on the limbs of the Talas–Fergana fault zone the displacement magnitude reaches 250 km. In the Southern Tian Shan the displacement along the strike-slip fault is reduced to 100 km [11].

### *Fergana horizontal flexure*

Folds and faults belonging to the second-collision deformation stage follow the Late Permian sinistral horizontal flexure on the western flank of the Talas–Fergana fault (Figs. 2, 8).

The southern limb of the flexure is formed by latitudinal structures of the Alai Range. The southern bend of the flexure represents horizontal fold (Fig. 8) with observable tectonic flow structures, formed due to extension of layers. Beds and units of limestone, chert, and sandstone are often boudinaged; boudins are spread laterally over a large distance. Signs of disharmonious deformation are commonly observed [13]. Structural forms resulting from the tectonic plastic flow have been studied at the meso- and microlevels in the study area [24].

The outer (eastern) area of the southern bend of the horizontal flexure is disharmonic relative to the inner zone. The core of the horizontal fold of the inner zone includes the Chilmairam tectonic block (Chil, Fig. 8a), wedge-shaped in plan and bounded by strike-slip fault zones. During the formation of horizontal folds this tectonic block was pushed in the northwesterly direction over a distance of 15–20 km or more [13, 20]. The core of the outer zone of the southern bend of the horizontal flexure is complicated by disharmonious horizontal second-order folds (the Akbogus horizontal fold, for example) (A, Fig. 8b). The latter is formed by nappes and recumbent isoclinal folds which were formed during the first stage of collision deformation and transformed into vertical folds during the second collision stage, and bent as a horizontal fold during the post-collision deformation stage. In addition, the Akbogus horizontal fold is structurally disharmonic in the core due to penetration of the material into its axial zone [13, 38].

The northern bend of the Fergana horizontal flexure is outlined by the axial line of the Maylisu synform (M, Fig. 8), arched in the westerly direction [9, 13, 14]. The length of the curved limb of the Fergana horizontal flexure is comparable with the Late Paleozoic dextral displacement on the Talas–Fergana strike-slip fault.

The geodynamics of the interaction between the Fergana horizontal flexure and the Talas–Fergana strike-slip fault is the subject of lively debate [3, 9, 13, 22, 26, 34, etc.]. The optimal solution to this problem is proposed in [23, 25], where the formation of the Fergana horizontal flexure is considered to be resulted from tectonic overflowing of rock masses of the Southern Tian Shan. According to this pattern, the Fergana horizontal flexure presents a large horizontal extrusion (protrusion), displaced in a northwesterly direction (Fig. 8c). From the northeast, this plastic flow was limited by the Talas–Fergana strike-slip fault. Accordingly, the formation of the horizontal extrusion is a consequence of the displacement of rock masses along the fault zone.

The extrusion pattern of the formation of the Fergana horizontal flexure is in agreement with the specific feature of the Talas–Fergana strike-slip fault, namely, the reduction in the displacement magnitude in the South Tian Shan was not accompanied by the formation of compensating tectonic structures. The Fergana horizontal flexure and the Talas–Fergana strike-slip fault may have been formed synchronously in the same stress field. The former could be younger than the latter, the fault plane of which could control the plastic flow.

In the Turkestan and Alai mountain ranges of the Southern Tian Shan, a sublatitudinal narrow high-strain zone was identified (Fig. 9a). The western part of the zone is called Nuratau–Kurganak, and the eastern part, Akmuinak [25]. The deformation-induced extension of some objects within this zone reaches 300–500%. The entire fold belt was probably subject to longitudinal extension elongation. The pattern of the development of the Late Permian deformations in the Western Tian Shan includes its lateral shortening as a result of meridionally oriented stress impact, the tectonic flow of the rock masses along the fold belt eastward, and their deposition as a giant extrusion, the Fergana horizontal flexure.

### *Junggar strike–slip fault*

The relationship between the Junggar fault (Fig. 1) and the tectonic structures of its limbs indicates dextral displacement of the rock mass. The same conclusion follows from the results of studying the micro-

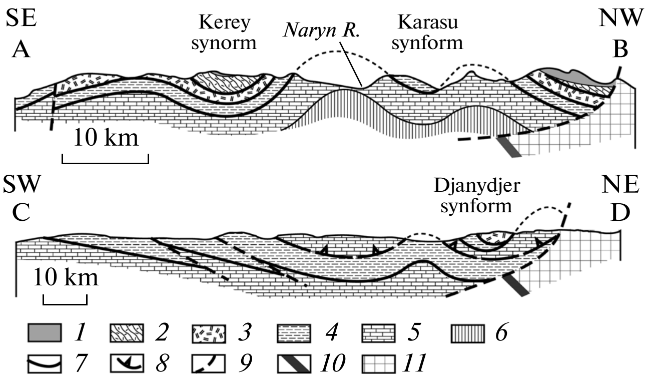


**Fig. 7.** Nappes, mapped along transects of AB (North Fergana area) and CD (Atbashi–Kokshaal area) (see Fig. 2). (*1*) neoautochthon; (*2*, *3*) accretionary-collision nappes: (*2*) Shaidan unit, (*3*) Kerey and Keltubek units, see Fig. 3); (*4*) collision nappes (units of Ontamchi, Chatyr Kul, and their counterparts); (*5*, *6*) autochthon and paraautochthon (units of Baubashata, Kokkija, and their counterparts): (*5*) Devonian and Carboniferous, (*6*) Silurian; (*7*) primary overthrust faults; (*8*) Borkoldoi secondary overthrust fault; (*9*) post-collision faults; (*10*) Turkestan oceanic suture; (*11*) Kazakh–Kyrgyz terrane.

structure of migmatites and milonitized schists and quartzites near the fault plane. The Ar–Ar age of mylonite from the fault zone varies in the range of 255–285 Ma [49]. The Ar–Ar ages of new mica from mylonite, probably formed as a result of shear displacement along the Junggar fault, are 270 and 245 Ma [65].

Most of the Junggar strike-slip fault runs along the West Junggar oceanic suture, which makes it difficult to determine the displacement magnitude of the fault. Since the prefault tectonic zones are separated along the Junggar fault over a distance of more than 200 km [14], it is difficult to estimate which part of this distance was shifted along the fault and which part indicates the primary strike of the tectonic zone along the oceanic suture and the future strike-slip fault. According to [46], the dextral shear displacement magnitude along the Chingiz–Alakol–Junggar fault in Late Permian to Early Triassic was estimated to be 490 ± 250 km. In the Permian shear displacements occurred also along longitudinal faults of the Tian Shan [48, 65, 72, 92, etc.].

During the post-collision stage within the Western, Central and, probably, Eastern Tian Shan the Alai–Tarim terrane was overthrust onto the Kazakh–Kyrgyz terrane, reaching a maximum magnitude at the extrusion of the Fergana horizontal flexure. As a result, the Permian thrust zone overlapping the Late Carboniferous Turkestan oceanic suture along its entire length has recently come to be regarded as a Turkestan oceanic suture (Figs. 2, 6, 7).

### *Deformation revealed by paleomagnetic analysis*

The paleomagnetic properties of Permian rocks (Fig. 9) were studied in many localities of the Tian Shan. Paleomagnetic declinations in Permian rocks of

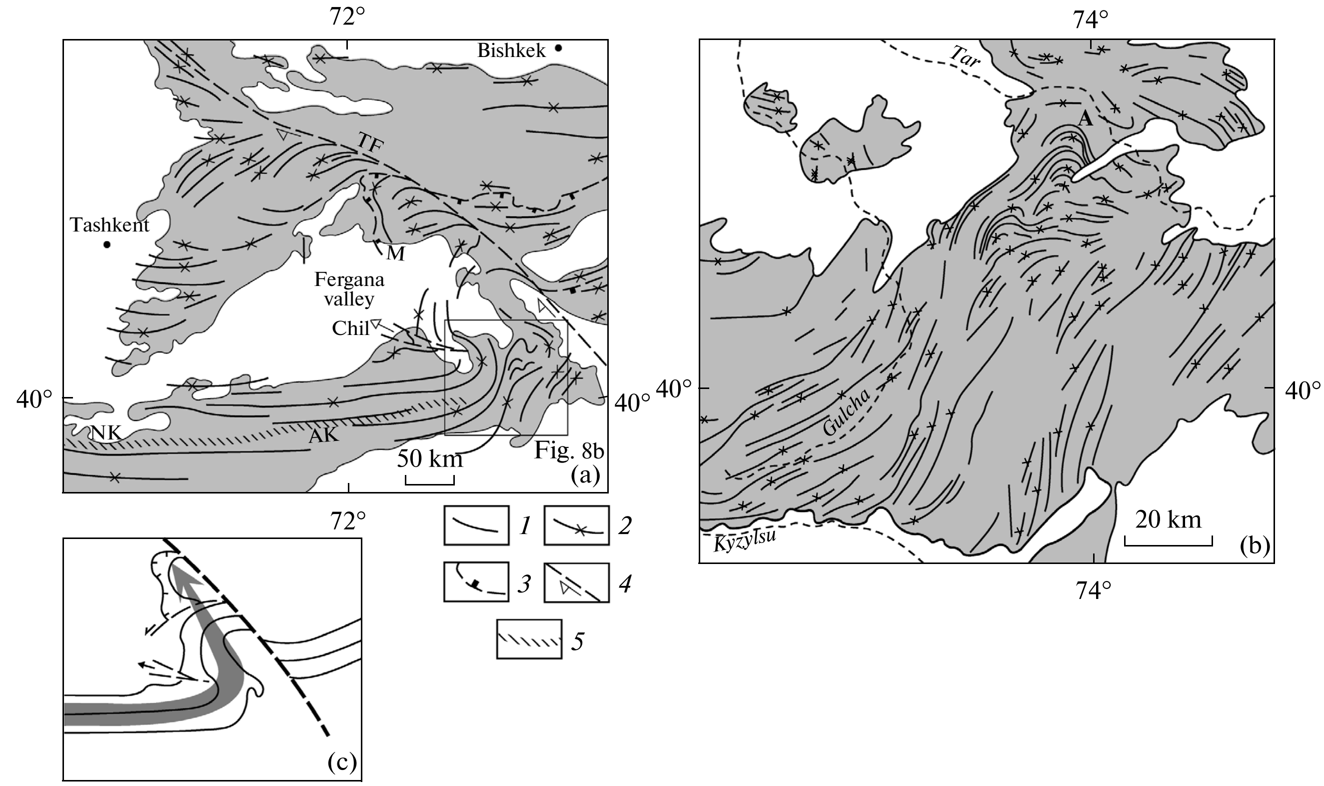


**Fig. 8.** Late Paleozoic folds in West Tian Shan: (a) general view; (b) southern bend of the Fergana horizontal flexure; (c) formation scheme of the Fergana flexure, tectonic movement is shown by wide arrow. (*1*, *2*) axial lines of vertical folds: (*1*) anticline and antiform, (*2*) syncline and synform; (*3*, *4*) major faults: (*3*) thrusts, (*4*) strike-slips; (*5*) high-strain zone (AK, Akmuinak; NK, Nuratau–Kurganak; A, Akbogus horizontal fold; M, axial line of the Maylisu fold; TF, Talas–Fergana fault; Chil, Chilmayram tectonic block). The distribution area of Paleozoic rocks (Figs. 8a and 8b) is shown in gray.

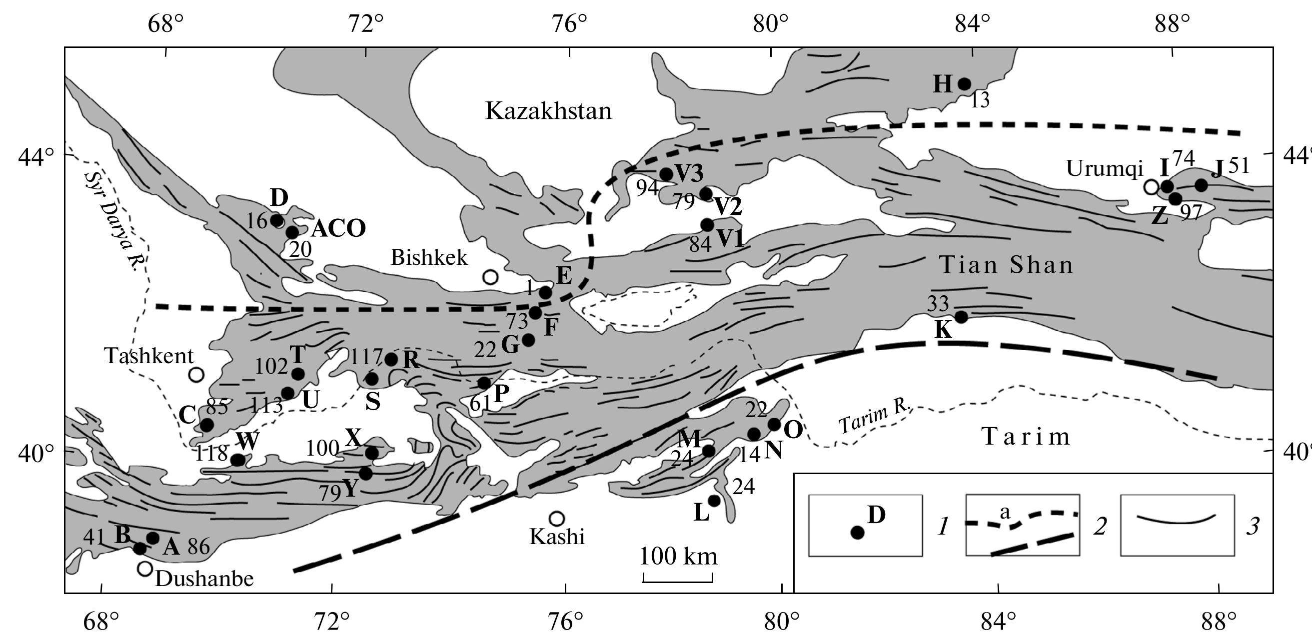


**Fig. 9.** The belt of Late Paleozoic sinistral deformations, modified after [37]. (*1*) Sites A–Z of paleomagnetic studies of Permian rocks: digits 1–118 mean rotation angles (in degrees) of the Permian paleomagnetic declination relative to direction towards the Permian paleomagnetic pole (table); (*2*) northern (a) and southern boundaries of the belt of sinistral deformations; (*3*) axial lines of Late Paleozoic folds. The distribution area of Paleozoic and pre-Paleozoic rocks is shown in gray.

the Tian Shan show counterclockwise rotation relative to the primary direction towards the Permian paleomagnetic pole (table). Measurements on the Tarim Platform–Tian Shan border (sites L, M, N, O, Fig. 9), and close to the Tian Shan–Kazakhstan border (sites ASO, D, E, and H) show that the rotation angles of paleomagnetic declinations are less than 25°; in the Tian Shan, rotation angles are higher. The rotation of the paleomagnetic declination may be caused by: (a) the rotation of the entire region, (b) intraregion deformations, accompanying by the rotation around the vertical or steeply inclined axis, or (c) a combination of the above processes.

The Permian paleomagnetic declination in the southern Tarim is rotated counterclockwise at an angle of 22° ± 11° [54], which is similar to the rotation angles in the North Tarim and South Kazakhstan. The distribution of paleomagnetic vectors througout the Tian Shan and adjacent areas allows us to draw the following conclusions: (a) the rotation of paleomagnetic declinations at an angle less than 25° is a consequence of the rotation of an extensive region or the entire continent in the post-Permian; (b) such a rotation angle, up to 25°, in the Tian Shan is a background of the paleomagnetic rotation in post-Permian; (c) the rotation of paleomagnetic declinations at angles higher than the background ones (25°) is a result of internal deformation in the Tian Shan fold belt.

Rotation of paleomagnetic declinations indicates a field of sinistral strike-slip deformations within the Tian Shan [37]. It could be rotation of small domains with sinistral strike-slip differential flow of the rock mass. The magnitudes of rotating domains and their boundaries are not established and this problem requires special study. Large differences between the rotation angle values in different parts of the belt of strike-slip deformations (Fig. 9) show the dependence of strain intensity on local conditions.

The paleomagnetism of Permian rocks was studied on two stratigraphic levels, the Sakmarian–Artinskian and the Kazanian (locality sites R, T, and U). Between these age levels, paleomagnetic declinations were rotated clockwise at an angle of 64° ± 18° in the locality site R, and 44° ± 14° in sites T, U. The rotation angle of the paleomagnetic declinations in these areas, including the background rotation and rotation in the post-Kazanian is more than 100°. Sites R and S are located within the Fergana horizontal flexure, and sites T and U are located in the zone of compensation thrusts and folds whose origin is associated with the formation of the flexure. It seems natural to connect the rotation of the paleomagnetic declinations in these locality sites with the formation of the Fergana extrusion. The results of studying the paleomagnetic properties of Permian rocks in locality sites R, T, and U confirm the proposed high activity of the extrusion process in the Late Early and Early Late Permian.

Deviation of paleomagnetic declinations in Permian rocks of Northern Tarim, Tian Shan, and Southern Kazakhstan relative to the direction of the Permian paleolongitude

| Locality site | R° | Source | Locality site | R° | Source |
|---|---|---|---|---|---|
| Northern Tarim | | | S | 117 ± 14 | [37] |
| L | 24 ± 7 | [37, 68] | T | 102 ± 8 | [37] |
| M | 24 ± 5 | [37, 80] | U | 113 ± 10 | [37] |
| N | 14 ± 11 | [36, 37] | V1 | 84 ± 7 | [85] |
| O | 22 ± 6 | [36, 37] | V2 | 79 ± 10 | [85] |
| Tian Shan: TSZSD | | | V3 | 94 ± 8 | [85] |
| A | 86 ± 5 | [37] | W | 118 ± 15 | [37] |
| B | 41 ± 6 | [37] | X | 100 ± 8 | [19] |
| C | 85 ± 4 | [10, 37] | Y | 79 ± 9 | [19] |
| F | 73 ± 8 | [37 ] | Z | 97 ± 7 | [48] |
| G | 22 ± 5 | [37] | Southern Kazakhstan | | |
| I | 74 ± 8 | [37, 79] | ACO | 20 ± 7 | [62] |
| J | 51 ± 10 | [37, 73] | D | 16 ± 4 | [37] |
| K | 33 ± 9 | [37, 71] | E | 1 ± 4 | [37] |
| P | 61 ± 10 | [37] | H | 13 ± 7 | [99] |
| R | 117 ± 15 | [37] | | | |

R° means deviation (counterclockwise, in degrees) of the paleomagnetic declination of the pre-folded magnetization component in Permian rocks relative to direction towards the Permian paleomagnetic pole. TSZSD means the Tian Shan zone of sinistral deformation. The locations of sections are shown in Fig. 9.

### *Post-Collision Sedimentation and Magmatism*

Most of the Turkestan sea was drained in the Early Permian, and only in the narrow zone stretching from Kepingtagh to Kuruktag along the Tarim Platform were fine-grained flysch and carbonate-siliceous marine sediments deposited in the Late Permian (Bilongleibaoguzi Formation [66]). In the post-Permian period, volcanic deposits and continental molasses were deposited in isolated localities within the Tian Shan. Molasse represented mostly by coarse-grained deposits continued to be deposited in the territory of the Tian Shan in the Early Triassic. The molasse deposits were dated based on the findings of paleoflora or freshwater paleofauna. In the Southern Tian Shan they compose the neoautochthon-3 (Fig. 3), which discordantly lies on different-aged rocks belonging to different allochthonous units and autochthon. Molasse accumulated in depressions and grabens due to erosion of local provenance areas.

Post-collision Permian magmatism in the Tian Shan is predominantly of alkaline composition and continental origin. Permian volcanic and volcanogenic sediments rest with angular nonconformity on Late Carboniferous and older rocks and often fill graben structures. These deposits reach a high thickness (up to 4 km) in the Chatkal–Kurama area of the Western Tian Shan. The basal volcanic rocks are represented by rhyolite, trachyrhyolite, trachydacite (Oysai and other formations). Further up the section, volcanic rocks are of more contrasting trachybasalt–trachyrhyolite composition (Shurabsai and other formations). The lower part

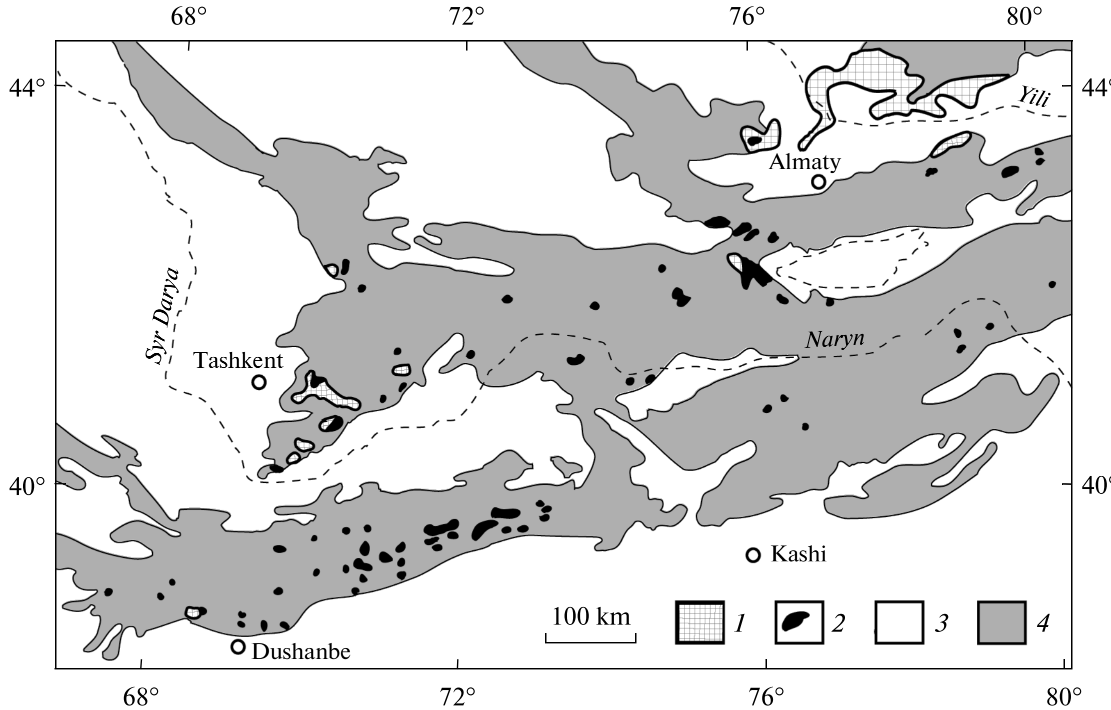


**Fig. 10.** Late Paleozoic alkaline and subalkaline magmatism in Western and Central Tian Shan. (*1*, *2*) Alkaline and subalkaline volcanic rocks (*1*) and intrusions (*2*); (*3*) Cenozoic; (*4*) Paleozoic.

of the section contains Asselian and Sakmarian fauna and flora; clastic rocks overlying volcanites contain Kazanian (Wordian) flora remnants [18]. The Rb–Sr isochron ages of lavas and comagmatic intrusions are in the range of 268–284 Ma [17, 18]; the Ar–Ar age of rhyolite is 292 Ma [17]; the U–Pb ages of granites are in the range of 275–300 Ma [78].

In the Trans-Yili–Ketmen ranges of the Central Tian Shan rocks with Late Carboniferous flora are overlain with the angular unconformity by a stratum of volcanic and sedimentary rocks of the Baskainar and other formations, containing Permian paleoflora [4]. In the lower part, the stratum is composed of lava and tuffs of basaltic, andesite–basaltic, and andesite compositions with high alkalinity. Further up the section, the amount of lavas decreases and that of tuff lava and tuffs increases. The latter becomes trachytic, trachyrhyolitic, and trachydacitic in composition. The upper part of the section is composed of red clastic rocks and trachyandesites. The proportion of alkaline rocks among volcanites decreases northward.

The U–Pb zircon ages of many granite massifs of Tian Shan are given in [8, 56, 70, 78, 86, 97]. There is no regularity in distributing the Permian granites that are attributable to S- and A-types. Due to a lack of data, the type of granite is often difficult to determine [8, 81]. Permian alkaline magmatism is probably confined to extension zones that developed during shear displacements within the Tian Shan strike-slip fault zone (Fig. 9). The locality map of Permian alkaline and subalkaline magmatism (Fig. 10) indicates that there were many local extension zones in the post-collision time.

The pattern of intraplate magmatism is violated at the Eastern Tian Shan–Tarim massif boundary. Here, in the Harkeshan Range piedmont, the Upper Carboniferous deposits are unconformably overlain by lavas and pyroclastics, reaching a thickness of several kilometers. Dacites and rhyolites are in predominance among lavas. The Ar–Ar age of lava is 282 ± 2 Ma, and the Rb–Sr age is 286 ± 17 Ma [44, 47]. Volcanic rocks are intruded by plagiogranite, adamellite, and granodiorite massifs. Rocks are of calc-alkaline composition. Geochemical parameters of lavas are evidence of their formation under subduction-related and collision settings. The calc-alkaline magmatism probably indicates that the rift oceanic basin existed in the Early Permian near the Tian Shan–Tarim boundary. The formation of this basin may be associated with mantle plume activity, caused the outpouring of plateau basalts on the Tarim massif in the Early Permian [32, 74].

## DISCUSSION AND CONCLUSIONS

The complex tectonics of the Tian Shan, the wide development of sedimentary and tectonic mixtites and signs of redeposition of fossil fauna lead to the fact that there remains room for doubt about the validity of conclusions having made and reliability of the data used for their justification. The factual data can be interpreted in a different way. All this allows scientists to accept or refute arguments based on the points of view of different researchers. In turn, it creates favorable conditions for the development of different tectonic and geodynamic patterns. The fold–thrust structure of the Southern Tian Shan provides a great opportunity for development of variation and alternative interpretation patterns. Geodynamic and kinematic patterns, which significantly differ from the above-discussed pattern are provided in [1, 5, 7, 25, 46, 69, 87, 91, etc.]. Let us consider some patterns proposed.

### *Subduction of the Turkestan oceanic crust*

According to most existing geodynamic models, the Turkestan margin of the Kazakh–Kyrgyz continent is active, the margin of the Alai–Tarim continent is passive, subducted by the oceanic crust beneath the Kazakh–Kyrgyz continent [7, 13, 14, 35, 38, 41, 47, 50, 52, 53, 61, 94, 96]. This scheme is based on widespread manifestations of the subduction-related magmatism within the Kazakh–Kyrgyz continent, while this type of magmatism is not established within most of the Turkestan margin of the Alai–Tarim continent.

Both margins of the Kazakh–Kyrgyz continent, Turkestan and Junggar, were active. The connection of the subduction-related magmatism and the Turkestan margin is distinctly observable in the Western and Central Tian Shan. In the Eastern Tian Shan, the Kazakh–Kyrgyz continent reduces in area. Under such circumstances, the connection of the magmatism with subduction in either active continental margin of the Kazakh–Kyrgyz continent is difficult to establish. In general, the establishment of such a connection is based on studying the geochemical variations of igneous rocks with increasing distance from oceanic sutures towards the continent. The scarce data available are mentioned above. When creating a geodynamic pattern it is possible to use the sources of subduction-related magmatism depending on of an author's point of view. Another complicating factor in the reconstruction is the geodynamic rearrangement of the Kazakh–Kyrgyz continental lithosphere in the Eastern Tian Shan due to the narrowing of the continent and the convergence of active margins. The character of the interaction of mantle processes in adjacent active margins is unknown.

The above-listed circumstances made it possible to develop geodynamic evolution patterns of Eastern Tian Shan, provided that the Turkestan margin of the Kazakh–Kyrgyz continent is passive, and the oceanic crust of the Turkestan Ocean subducted beneath the Alai–Tarim continent [45, 46, 69, 87].

### *Kinematics of Collision Deformation*

The thrust nappes of the Tian Shan comprise oceanic crustal rocks, including exhumed high-pressure eclogites. This indicates that the root zones of such nappes are confined to the suture zone of an oceanic basin. Kinematic models taking into account the displacement of primary thrust nappes from one or two to three Late Paleozoic root zones are proposed.

(I) According to this pattern, the root zone of the primary thrusts is located close to the Tian Shan–Tarim Craton boundary, from whence the nappe thrusts moved northward [45, 46, 65]. The results of studying the meso- and microstructures in metamorphic rocks argue for the northern direction of movement of nappe thrusts. These rocks are likely to belong to upper level nappes. They were subject to metamorphism and deformation, having been a part of the Middle Paleozoic accretionary prism at the Turkestan margin of the Kazakh–Kyrgyz continent, where the underthrustung and overthrusting of tectonic plates were directed northward towards this continent in modern coordinates. Conclusions about the character of the deformations in the accretionary prism cannot be applied to the simulation of the formation of the above-described ensemble of nappe thrusts, which occurred later, after the closure of the Turkestan oceanic basin. The thrusts intersecting the multilevel ensemble of nappes, folds, and paleonappes, which were formed in the Permian during the second collision deformation stage after the ensemble of nappes was formed, are mentioned above in the text. These structural forms are often of the northern vergence that makes the primary movement direction of the nappes undistinguishable.

(II) The authors of this pattern suggest that there was a counter movement of nappes from root zones, one of which is located in the north (the suture of the Turkestan paleoocean), the other, or others, in the south, near the borders of the Tian Shan with the Tarim craton and the Karakum terrane [1, 5, 7, 27].

(III) This pattern is described in this article. We consider the suture of the Turkestan paleoocean as a root zone of primary nappes of Southern Tian Shan. This is confirmed by the following data: the directions of the primary nappes determined by studying the tectonic vergence of folds within tectonic nappes [1, 12–14, 41]; the age of olistostromes and molasses [7, 14, 41]; and the age and consequence of movements of nappes [14, 41]. This pattern is in good agreement with the conclusions that the Turkestan oceanic crust subducted beneath the Kazakh–Kyrgyz continent, followed by the subduction of the Alai–Tarim continental terrane in Late Carboniferous beneath the same continent. These conclusions are confirmed by the wide distribution of subduction-related magmatism products beneath the Kazakh–Kyrgyz terrane.

The analysis of geodynamic and kinematic patterns of the tectonic evolution of the Tian Shan in the Middle and Late Paleozoic allows us to make the following conclusions:

(1) The subduction of the Turkestan paleooceanic crust beneath the Alai–Tarim continent and formation of nappes, following pattern I, is hardly probable.

(2) Evolution following pattern II is probable, but there is still no structural evidence of the displacement of primary nappes in the northern direction and the southern root zones of nappes have not been traced and studied.

(3) Pattern III corresponds to the available data.


## ACKNOWLEDGMENTS

I am grateful to D.V. Alekseev for his useful comments on the article.


## REFERENCES


1. D. V. Alekseev, Yu. S. Biske, V. Bo, et al., "Tectonostratigraphic framework and Palaeozoic evolution of the Chinese South Tianshan," Geotectonics **49**, 93–122 (2015).
2. R. Akhundzhanov, S. S. Saidyganiev, and L. I. Khamrabaeva, "Rb–Sr age, melt sources, and ore potential of Middle Paleozoic magmatic formations of the Almalyk–Angren mining region," Geol. Miner. Resur. (Tashkent), No. 3, 42–53.
3. A. B. Bakirov, "On the character of tectonic motions in the mountain framing of the Fergana in Late Paleozoic," in *Tectonics of Western Areas of Northern Tian Shan*, Ed. by M. M. Adyshev and V. G. Korolev (Ilim, Frunze, 1964), pp. 35–46.
4. G. R. Bekzhanov, V. Ya. Koshkin, I. I. Nikitchenko, et al., *Geological Structure of Kazakhstan* (Akad. Min. Res., Almaty, 2000) [in Russian].
5. Yu. S. Biske, *Paleozoic Structure and Evolution of Southern Tian Shan* (S.-Peterb. Gos. Univ., St. Petersburg, 1996) [in Russian].
6. Yu. S. Biske, "Eastern (Chinese) sector of the Southern Tien Shan: Collisional structure and main features of its Paleozoic evolution," Vestn. S.-Peterb. Univ., Ser. 7: Geol., Geogr., No. 21, 3–13 (1998).
7. Yu. S. Biske, *Folded Regions of Northern Eurasia: Tian Shan Fold System* (S.-Peterb. Gos. Univ., St. Petersburg, 2006) [in Russian].
8. Yu. S. Biske, D. L. Konopel'ko, and R. Zel'tmann, "Geodynamics of Late Paleozoic magmatism in the Tian Shan and Its framework," Geotectonics **47**, 291–310 (2013).
9. Yu. S. Biske, G. S. Porshnyakov, and Yu. A. Talashmanov, *Herzinides of the Fergana Range and Adjacent Areas of Southern Tian Shan* (Leningr. Gos. Univ., Leningrad, 1982) [in Russian].
10. A. S. Bol'shakov, G. M. Solodovnikov, and Yu. K. Vinogradov, "Paleointensity of the geomagnetic field in the Early Permian," Phys. Solid Earth, No. 7, 70–77, (1989).
11. V. S. Burtman, *Talas-Fergana Strike-Slip Fault* (Nauka, Moscow, 1964) [in Russian].
12. V. S. Burtman, *Geology and Mechanics of Nappes* (Nedra, Moscow, 1973) [in Russian].
13. Burtman, V.S., *Structural Evolution of Paleozoic Fold Systems* (Nauka, Moscow, 1976) [in Russian].
14. V. S. Burtman, *Tien Shan and High Asia: Paleozoic Tectonics and Geodynamics* (GEOS, Moscow, 2006) [in Russian]. http://www.ginras.ru/struct/21/10/burtman.php
15. V. S. Burtman, "Tien Shan, Pamir, and Tibet: History and geodynamics of Phanerozoic oceanic basins," Geotectonics **44**, 388–404 (2010).
16. V. S. Burtman, *Tien Shan and High Asia: Cenozozic Geodynamics*, (Geos, Moscow, 2012) [in Russian]. http://www.ginras.ru/struct/21/10/burtman.php
17. V. N. Volkov, Yu. V. Gol'tsman, M. M. Arakelyants, G. T. Tadzhibaev, and D. Z. Zhuravlev, "Radiometric age of high-silicic volcanism in late orogenic troughs of the Chatkal–Kurama zone, Central Tien Shan," Stratigr. Geol. Correlation **5** (1), 79–95 (1997).
18. *Geology and Mineral Resources of the Republic of Uzbekistan*, Ed by T.Sh. Shayakubov and T.N. Dalimov (Universitet, Tashkent, 1998) [in Russian].
19. A. V. Dvorova and M. L. Bazhenov, "Paleomagnetism of Permian deposits of the eastern part of Southern Tien Shan," in *Paleomagnetism and Magnetism of Rocks*, Ed. by V.P. Shcherbakov, (SOLO, St. Petersburg, 2012), pp. 51–52 [in Russian].
20. A. V. Dronov, "Tectonic nappes of Osh Mountains," Byull. Mosk. O-va. Ispyt. Prir., Otd. Geol. Otd. Geol. **66** (3), 26–39 (1991).
21. V. V. Kiselev, "U–Pb zircon geochronology of magmatic formations of Northern Tien Shan," in *Problems of Geology and Geography of Kyrgyzstan* Ed. by A.B. Bakirov and A.N. Dikikh (Ilim, Bishkek, 1999), pp. 21–33.
22. V. L. Klishevich, Yu. S. Rzhevskii, A. N. Khramov, Yu. A. Talashmanov, and T. N. Krylova, "Late Variscan Horizontal Deformations in the Fergana Sector of Tien Shan," *Vestn. Leningr. Univ., Ser. 7: Geol., Geogr.*, No. 7, 3–10, (1989).
23. V. G. Konygin and M. G. Leonov, "Origin of the East Alay sigmoid," Dokl. Akad. Nauk SSSR **282**, 675–679 (1985).
24. V. G. Konygin and M. G. Leonov, "Tectonics of the Sugut metamorphic block, South Tien Shan," Byull. Mosk. O-va. Ispyt. Prir., Otd. Geol. **62** (6), 19–35 (1987).
25. M. G. Leonov, *Tectonics of Consolidated Crust* (Nauka, Moscow, 2008) [in Russian].
26. M. G. Lomize, "Fergana sigmoid and Talas-Fergana strike-slip fault in a collision structure of Central Asia," Dokl. Earth Sci. **350**, 1100–1103 (1996).
27. G. S. Porshnyakov, *Hercynides of Altay and Adjacent Areas of Southern Tien Shan* (Leningr. Gos. Univ., Leningrad, 1973) [in Russian].
28. G. S. Porshnyakov, "Formation stages of tectonic structures in different segments of the Southern Tian Shan Hercynides," in *Tectonics of Tian Shan and Pamir*, Ed. by I.E. Gubin and S.A. Zakharov (Nauka, Moscow, 1983), pp. 66–73 [in Russian].
29. I. I. Pospelov, "Formations and tectonic evolution of Variscides in the Southern Tian Shan and Northern Pamir," in *Early Geosynclinal Formations and Structures,* Ed. by Yu.M. Pushcharovskii and I.V. Khvorova, (Nauka, Moscow, 1987), pp. 149–178 [in Russian].
30. V. A. Simonov, K. C. Sakiev, N. I. Volkova, et al., "Conditions of formation of the Atbashy Ridge eclogites

(South Tien Shan)," Russ. Geol. Geophys. **49**, 803–815 (2008).

31. L. I. Skrinnik, "Post-Silurian tectonic evolution of Southeast Kazakhstan," Geotectonics **37**, 232–244 (2003).
32. E. V. Khristov, "Transition Middle Paleozoic section on the northern slope of the Moldotau Range and its position in the regional structure of Tian Shan," in *Tectonics of Pre-Paleozoic and Paleozoic Strata of Tian Shan*, Ed. by V.I. Knauf (Ilim, Frunze, 1970), pp. 125–142 [in Russian].
33. C. Y. Jiang, Y. Z. Li, P. B. Zhang, and S. F. Ye, "Petrogenesis of Permian basalts of the western margin of the Tarim Basin (China)," Russ. Geol. Geophys. **47**, 237–248 (2006).
34. D. V. Alexeiev, H. E. Cook, V. M. Buvtyshkin, and L. Y. Golub, "Structural Evolution of the Ural–Tian Shan Junction: a View from Karatau Ridge, South Kazakhstan," Comptes Rendus Geosci., Ed. by K. Schulmann, R. Scrivener, and J. M. Lardeaux, **341**, 287–297 (2009).
35. M. B. Allen, B. F. Windley, and C. Zhang, "Paleozoic collisional tectonics and magmatism of the Chinese Tien Shan, Central Asia," Tectonophysics **220**, 89–115 (1993).
36. Y. Bai, G. Chen, Q. Sun, Y. Sun, Y. Li, Y. Dong, and D. Sun, "Late Paleozoic polar wander path for the Tarim Platform and its tectonic significance," Tectonophysics **139**, 145–153 (1987).
37. M. L. Bazhenov, V. S. Burtman, and A. V. Dvorova, "Permian paleomagnetism of the Tien Shan: Succession and style of tectonic deformation," Tectonophysics **312**, 303–329 (1999).
38. V. S. Burtman, "The structural geology of Variscan Tien Shan, USSR," Am. J. Sci. **275-A**, 157–186 (1975).
39. V. S. Burtman, "Faults of Middle Asia," Am. J. Sci. **280**, 725–744 (1980).
40. V. S. Burtman, "The Tien Shan Early Paleozoic tectonics and geodynamics," Russ. J. Earth Sci., **8** (3), 1–23 (2006).
41. V. S. Burtman, "Nappes of the Southern Tien Shan," Russ. J. Earth Sci., **10**, ES1006 (2008). doi:10.2205/2007ES000223
42. V. S. Burtman and P. Molnar, "Geological and geophysical evidence for deep subduction of continental crust beneath the Pamir," Vol. 281 of *Geol. Soc. Am. Spec. Pap.*, (Geol. Soc. Am., Boulder, 1993).
43. V. S. Burtman, S. F. Scobelev, and P. Molnar, "Late Cenozoic slip on the Talas-Ferghana Fault, Tien Shan, Central Asia," Geo-Mar. Lett. **108**, 1004–1021 (1996).
44. A. R. Carroll, S. A. Graham, M. S. Hendrix, et al., "Late Paleozoic tectonic amalgamation of Northwestern China: Sedimentary record of the Northern Tarim, Northwestern Turpan and Southern Junggar basins," Geol. Soc. Am. Bull. **107**, 571–594 (1995).
45. J. Charvet, L. Shu, and S. Laurent-Charvet, "Paleozoic structural and geodynamic evolution of Eastern Tianshan (NW China): Welding of the Tarim and Junggar plates," Episodes **30**, 162–186 (2007).
46. J. Charvet, L. Shu, S. Laurent-Charvet, B. Wang, M. Faure, D. Cluzel, Y. Chen, and K. De Jong, "Palaeozoic tectonic evolution of the Tianshan Belt, NW China," Sci. China. Earth Sci. **54**, 166–184 (2011).
47. C. Chen, H. Lu, D. Jia, D. Cai, and S. Wu, "Closing history of the Southern Tianshan oceanic basin, Western China: An oblique collisional orogeny," Tectonophysics **302**, 23–40 (1999).
48. F. Choulet, Y. Chen, B. Wang, M. Faure, D. Cluzel, J. Charvet, W. Lin, and B. Xu, "Late Paleozoic paleogeographic reconstruction of Western Central Asia based upon paleomagnetic data and its geodynamic implications," J. Asian Earth Sci. **42**, 867–884 (2011).
49. K. De-Jong, B. Wang, M. Faure, L. Shu, D. Cluzel, J. Charvet, G. Ruffet, and Y. Chen, "New $^{40}Ar/^{39}Ar$ age constraints on the Late Palaeozoic tectonic evolution of the Western Tianshan (Xinjiang, Northwestern China), with emphasis on Permian fluid ingress," Int. J. Earth. Sci. **98**, 1239–1258 (2009).
50. Y. Dong, G. Zhang, F. Neubauer, X. Liu, J. Genser, and C. Hauzenberger, "Syn- and post-collisional granitoids in the Central Tianshan orogen: Geochemistry, geochronology and implications for tectonic evolution," Gondwana Res. **20**, 568–581 (2011).
51. J. Gao and R. Klemd, "Formation of HP-LT rocks and their tectonic implications in the Western Tianshan Orogen, NW China: Geochemical and age constraints," Lithos **66**, 1–22 (2003).
52. J. Gao, M. Li, X. Xiao, Y. Tang, and G. He, "Paleozoic tectonic evolution of the Tianshan orogen, northwestern China," Tectonophysics **287**, 213–231 (1998).
53. J. Gao, L. Long, R. Klemd, Q. Qian, D. Liu, X. Xiong, W. Su, W. Liu, Y. Wang, and F. Yang, "Tectonic evolution of the South Tianshan orogen and adjacent regions, NW China: Geochemical and age constraints of granitoid rocks," Int. J. Earth Sci. **98**, 1221–1238 (2009).
54. S. A. Gilder, X. X. Zhao, R. S. Coe, Z. Meng, V. Courtillot, and J. Besse, "Paleomagnetism and tectonics of the Southern Tarim basin, Northwest China," J. Geophys. Res. **101**, 22 015–22 031 (1996).
55. B. Han, Z. Guo, Z. Zhang, L. Zhang, J. Chen, and B. Song, "Age, geochemistry, and tectonic implications of a Late Paleozoic Stitching pluton in the North Tian Shan Suture Zone, Western China," Geol. Soc. Am. Bull. **122**, 627–640 (2010).
56. B. Han, G. He, X. Wang, and Z. Guo, "Late Carboniferous collision between the Tarim and Kazakhstan-Yili terranes in the western segment of the South Tian Shan Orogen, Central Asia, and implications for the Northern Xinjiang, Western China," Earth-Sci. Rev. **109**, 74–93 (2011).
57. E. Hegner, R. Klemd, A. Kröner, et al., "Mineral ages and P-T conditions of Late Paleozoic high-pressure eclogite and provenance of melange sediments from Atbashi in the South Tianshan orogen of Kyrgyzstan," Am. J. Sci. **310**, 916–950 (2010).
58. C. Hopson, J. Wen, G. Tilton, Y. Q. Tang, B. Q. Zhu, and M. Zhao, "Paleozoic plutonism in East Junggar. Bogdashan and Eastern Tianshan, NW China," EOS, Trans., Am. Geophys. Union **70**, 1403–1404 (1989).
59. K. J. Hsu, Y. Yao, J. Hao, P. Hsu, J. Li, and Q. Wang, "Origin of Chinese Tianshan by arc-arc collisions," Eclogae Geol. Helv. **87**, 365–392 (1994).

60. R. J. Jenchuraeva, "Paleozoic geodynamics, magmatism and metallogeny of the Tien Shan" in *Paleozoic Geodynamics and Gold Deposits in the Kyrgyz Tien Shan, IGCP-373, Publ. 18*, Ed. by R. Seltmann and R. Jenchuraeva, (R. Soc., London, 2001), pp. 29–70.

61. W. Ju and G. Hou, "Late Permian to Triassic intraplate orogeny of the southern Tianshan and adjacent regions, NW China," Geosci. China (2013). http://dx.doi.org/10.1016/j.gsf.2013.03.001

62. U. Kirscher, A. Zwing, D. V. Alexeiev, A. Mikolaichuk, and V. Bachtadse, "Paleomagnetism of Paleozoic sedimentary rocks from the Karatau Range, Southern Kazakhstan: Multiple remagnetization events correlate with phases of deformation," J. Geophys. Res.: Solid Earth **118**, 3871–3885 (2013).

63. R. Klemd, M. Brocker, B. R. Hacker, J. Gao, P. Gans, and K. Wemmer, "New age constraints on the metamorphic evolution of the high-pressure/low-temperature belt in the Western Tianshan Mountains, NW China," J. Geol. **113**, 157–168 (2005).

64. R. Klemd, T. John, E. E. Scherer, S. Rondenay, and J. Gao, "Changes in dip of subducted slabs at depth: Petrological and geochronological evidence from HP-UHP rocks (Tianshan, NW-China)," Mar. Geol. **310**, 9–20 (2011).

65. S. Laurent-Charvet and J. Charvet, "Late Paleozoic strike-slip shear zones in Eastern Central Asia (NW China): New structural and geochronological data," Tectonics **22**, 1099–1123 (2003).

66. K. Y. Lee, *Geology of the Tarim Basin with Special Emphasis on Petroleum Deposits, Xinjiang Uygur Zizhiqu, Northwest China (U.S. Geol. Open-File Rep. 85-0616)*, (1985).

67. Q. L. Li, W. Lin, W. Su, X. H. Li, Y. H. Shi, Y. Liu, and G. Q. Tang, "SIMS U-Pb rutile age of low-temperature eclogites from Southwestern Chinese Tianshan, NW China," Lithos **122**, 76–86 (2011).

68. Y. P. Li, M. McWilliams, A. Cox, R. Sharps, Y. Li, Z. Gao, Z. Zhang, and Y. Zhai, "Late Permian paleomagnetic pole from dikes of the Tarim Craton," Geology **16**, 275–278 (1988).

69. W. Lin, M. Faure, Y. Shi, Q. Wang, and Zh. Li, "Paleozoic tectonics of Southwestern Chinese Tianshan: New insights from a structural study of the high-pressure/low-temperature metamorphic belt," Intern. J. Earth Sci. **98**, 1259–1274 (2009).

70. L. Long, J. Gao, R. Klemd, C. Beier, Q. Qian, X. Zhang, J. Wang, and T. Jiang, "Geochemical and geochronological studies of granitoid rocks from the Western Tianshan orogen: implications for continental growth in the Southwestern Central Asian orogenic belt," Lithos **126**, 321–340 (2011).

71. P. L. McFadden, X. H. Ma, M. H. McElhinny, and Z. K. Zhang, "Permo-Triassic magnetostratigraphy in China: Northern Tarim," Mar. Geol. **87**, 152–160 (1988).

72. A. V. Mikolaichuk, "The Late Paleozoic strike-slip assemblies and their influence on the Tien Shan Cenozoic framework," in *Geodynamics of the Tien Shan*, (Bishkek, 2000), pp. 64–67.

73. S. Y. Nie, D. B. Rowley, R. Van der Voo, and M. S. Li, "Paleomagnetism of Late Paleozoic rocks in the Tianshan, Northwestern China," Tectonics **12**, 568–579 (1993).

74. K. Qin, B. Su, S. P. Asamoah, D. Tang, X. Li, H. Sun, Q. Xiao, and P. Liu, "SIMS zircon U-Pb geochronology and Sr-Nd isotopes of Ni-Cu-bearing mafic-ultramafic intrusions in Eastern Tianshan and Beishan in correlation with flood basalts in Tarim Basin (NW China): Constraints on a ca 280 Ma mantle plume," Am. J. Sci. **311**, 237–260 (2011).

75. *Regional Geology of Xinjiang Uygur Autonomous Region* (Geol. Publ. House, Beijing, 1993 [in Chinese and English].

76. E. A. Rogozhin, "Morphology and origin of Folding in the South Tien Shan," Rus. J. Earth Sci. **6** 1 (2004).

77. Y. Rolland, D. V. Alexeiev, A. Kroner, M. Corsini, C. Loury, and P. Monié, "Late Palaeozoic to Mesozoic kinematic history of Talas-Ferghana strike-slip fault (Kyrgyz West Tianshan) revealed by a structural study and $^{40}Ar/^{39}Ar$ dating," J. Asian Earth Sci. **67–68**, 76–92, (2013).

78. R. Seltmann, D. Konopelko, G. Biske, F. Divaev, and S. Sergeev, "Hercynian post-collisional magmatism in the context of Paleozoic magmatic evolution of the Tien Shan orogenic belt," J. Asian Earth Sci. **42**, 821–838 (2011).

79. R. Sharps, Y. P. Li, M. McWilliams, and Y. Li, "Paleomagnetic investigation of Upper Permian sediments in the South Junggar Basin, China," J. Geophys. Res. **97** 1753–1765 (1992).

80. R. Sharps, M. O. McWilliams, Y. P. Li, A. Cox, Z. Zhang, Y. Zhai, Z. Gao, Y. Li, Q. Li, "Lower Permian paleomagnetism of the Tarim block, Northwestern China," Mar. Geol. **92**, 275–291 (1989).

81. L. I. Solomovich and B. A. Trifonov, "Postcollisional magmatism in the South Tien Shan Variscan orogenic belt, Kyrgyzstan: Evidence for high-temperature and high-pressure collision," J. Asian Earth Sci. **30**, 142–153 (2007).

82. W. Su, J. Gao, R. Klemd, J. Li, X. Zhang, X. Li, N. Chen, and L. Zhang, "U-Pb zircon geochronology of Tianshan eclogites in NW China: Implication for the collision between the Yili and Tarim blocks of the Southwestern Altaids," Eur. J. Mineral **22**, 473–478 (2010).

83. M. Tagiri, T. Yano, A. Bakirov, T. Nakajima, and S. Uchiumi, "Mineral parageneses and metamorphic P-T paths of ultrahigh-pressure eclogites from Kyrghyzstan Tien-Shan," Island Arc **4**, 280–292 (1995).

84. G. Tang, Q. Wang, D. A. Wyman, Z. Li, Z. Zhao, and Y. Yang, "Geochronology and geochemistry of Late Paleozoic magmatic rocks in the Lamasu-Dabate area, Northwestern Tianshan (West China): Evidence for a tectonic transition from arc to post-collisional setting," Lithos **119**, 393–411 (2010).

85. R. Van der Voo, N. M. Levashova, L. S. Skrinnik, T. V. Kara, and M. L. Bazhenov, "Late orogenic, large-scale rotations in the Tien Shan and adjacent mobile belts in Kyrgyzstan and Kazakhstan," Tectonophysics **426**, 335–360 (2006).

86. B. Wang, D. Cluzel, L. Shu, M. Faure, J. Charvet, Y. Chen, S. Meffre, and K. de Jong, "Evolution of calc-alkaline to alkaline magmatism through Carboniferous

convergence to Permian transcurrent tectonics, Western Chinese Tianshan," Intern. J. Earth Sci. **98**, 1275 – 1298 (2009).

87. B. Wang, M. Faure, L. Shu, K. De Jong, J. Charvet, D. Cluzel, B. Jahn, Y. Chen, and G. Ruffet, "Paleozoic tectonic evolution of the Yili Block, Western Chinese Tianshan," Bull. Soc. Geol. Fr., **179**, 483–490 (2008).
88. B. Wang, M. Faure, L. Shu, K. De Jong, J. Charvet, D. Cluzel, B. Jahn, Y. Chen, and G. Ruffet, "Structural and geochronological study of high-pressure metamorphic rocks in the Kekesu Section (Northwestern China): Implications for the Late Paleozoic tectonics of the Southern Tianshan," J. Geol. **118**, 59–77 (2010).
89. B. Wang, Z. Lang, X. Li, et al., *Comprehensive Survey of Geological Sections of the West Tianshan of Xinjiang, China* (Urumqi, 1994) [in Chinese and English].
90. B. Wang, L. Shu, D. Cluzel, M. Faure, and J. Charvet, "Geochemical constraints on Carboniferous volcanic rocks of Yili Block (Xinjiang, NW China): Implication for the tectonic evolution of Western Tianshan," J. Asian Earth Sci. **29**, 148–159 (2007).
91. Q. Wang, L. Shu, J. Charvet, M. Faure, H. Ma, B. Natal'in, J. Gao, A. Kroner, W. Xiao, J. Li, B. Windley, Y. Chen, R. Glen, P. Jian, W. Zhang, R. Seltmann, S. Wilde, F. Choulet, B. Wan, C. Quinn, Y. Rojas-Agramonte, Q. Shang, W. Zhang, B. Wang, and W. Lin, "Understanding and study perspectives on tectonic evolution and crustal structure of the Paleozoic Chinese Tianshan," Episodes **33**, 242–266 (2010).
92. Y. Wang, J. Li, and G. Sun, "Postcollisional eastward extrusion and tectonic exhumation along the Eastern Tianshan Orogen, Central Asia: Constraints from dextral strike-slip motion and $^{40}Ar$-$^{39}Ar$ geochronological evidence," J.Geol. **116**, 599–618 (2008).
93. Z. Wang, J. Wu, X. Lu, et al., *Polycyclic Tectonic Evolution and Metallogeny of the Tianshan Mountains* (Science Press, Beijing, 1990).
94. B. F. Windley, D. Alexeiev, W. Xiao, A. Kröner, and G. Badarch, "Tectonic Models for Accretion of the Central Asian Orogenic Belt," J. Geol. Soc. London **164**, 31–47 (2007).
95. L. Xia, X. Xu, Z. Xia, X. Li, Z. Ma, and L. Wang, "Petrogenezis of Carboniferous rift-related volcanic rocks in the Tienshan, Northwestern China," Bull. Geol. Soc. Am. **116**, 419–433 (2004).
96. W. Xiao, B. F. Windley, M. B. Allen, and C. Han, "Paleozoic multiple accretionary and collisional tectonics of the Chinese Tianshan orogenic collage," Gondwana Res. **23**, 1316–1341 (2013).
97. C. Zhang, Z. Li, X. Li, Y. Xu, G. Zhou, and H. Ye, "A Permian large igneous province in Tarim and Central Asian orogenic belt, NW China: Results of a ca. 275 Ma mantle plume?" Geol. Soc. Am. Bull. **122**, 2020–2040 (2010).
98. L. Zhang, Y. Ai, and S. Song, "A brief review of UHP meta-ophiolitic rocks, Southwestern Tianshan, Western China," Intern. Geol. Rev. **49**, 811–823 (2007).
99. X. Zhao, R. S. Coe, Y. Zhou, H. Wu, and J. Wang, "New paleomagnetic results from Northern China: Collision and suturing with Siberia and Kazakhstan," Tectonophysics **181**, 43–81 (1990).

*Reviewer M.G. Leonov*
*Translated by D. Voroshchuk*